

Long carrier lifetimes in GaN epitaxial layers grown using TiN porous network templates

Ü. Özgür,^{a)} Y. Fu, Y. T. Moon, F. Yun, and H. Morkoç

Department of Electrical Engineering, Virginia Commonwealth University, Richmond, Virginia 23284

H. O. Everitt^{b)}

Department of Physics, Duke University, Durham, North Carolina 27708

S. S. Park and K. Y. Lee

Samsung Advanced Institute of Technology, P.O.Box 111, Suwon, Korea 440-600

Abstract

Improved structural quality and radiative efficiency were observed in GaN thin films grown by metalorganic chemical vapor deposition (MOCVD) on TiN porous network templates formed by in-situ thermal annealing of Ti in ammonia. The room temperature decay times obtained from biexponential fits to time-resolved photoluminescence data are longer than ever reported for GaN. The carrier lifetime of 1.86 ns measured for a TiN network sample is slightly longer than that for a 200 μm -thick high quality freestanding GaN. The linewidth of the asymmetric X-Ray diffraction (XRD) $(10\bar{1}2)$ peak decreases considerably with the use of TiN layer and with increasing in-situ annealing time, indicating the reduction in threading dislocation density. However, no direct correlation is yet found between the decay times and the XRD linewidths, suggesting that point defect and impurity related nonradiative centers are the main parameters affecting the lifetime.

^{a)} Electronic mail: uozgur@vcu.edu

^{b)} Also with the U.S. Army Research Office, Research Triangle Park, Durham, NC 27709

Technological advances in group-III nitride-based optoelectronic and electrical devices have been made possible owing to extensive materials research, resulting in the commercialization of short wavelength emitters and detectors.¹ Meanwhile, the motivation for improved devices as well as bringing high performance electronic devices to the market place is continually driving the GaN technology for improved material quality with better optical and electrical performance. Conventional heteroepitaxial growth of GaN on low-temperature GaN or AlN buffer layers deposited on sapphire (Al_2O_3) and SiC substrates results in films containing high density of threading dislocations (TDs) (10^9 - 10^{10} cm^{-2}) and associated point defects due to lattice mismatch between the film and the substrate. These imperfections affect both the optical and electrical properties, hindering the advances in device performance since they scatter charge carriers and hamper the efficiency of radiative recombination.²

The best quality GaN epilayers are obtained by using homoepitaxial growth over freestanding GaN templates or bulk GaN; however, at present, the size and growth rate of high quality bulk crystals are limited. Thick hydride vapor phase epitaxy (HVPE) -grown GaN templates exhibit very low TD densities (5×10^6 cm^{-2}).^{3,4} For the reduction of TDs and to obtain device-quality GaN epilayers, different methods such as epitaxial lateral overgrowth (ELO)⁵ and micro-ELO on *in-situ* grown discontinuous SiN_x layer mask^{6,7,8} are introduced. The ELO process requires ex-situ photolithographic preparation that is cumbersome and increases the cost. In this paper, we report on the optical characterization of thin GaN epitaxial layers grown by metalorganic chemical vapor deposition (MOCVD) on TiN micro-porous networks. The photogenerated carrier decay times measured by time-resolved photoluminescence (TRPL) are longer than ever reported and are shown to be

larger than that for a thick HVPE-grown template and thin films without the TiN network: an indication of the superior quality of the overgrown GaN layers.

Ti films of 10 nm were e-beam evaporated on 0.7 μm -thick MOCVD-grown GaN templates, and then subjected to in-situ thermal annealing at 1050 $^{\circ}\text{C}$ in a fixed ratio of NH_3 to H_2 (1:3) gases inside the MOCVD chamber at 200 Torr. Critical parameters for TiN annealing conditions such as the gas ratio (H_2 : NH_3 , with a constant total flow rate), annealing temperature, and annealing time had been explored previously.⁹ Annealing times of 15, 30, 45, and 60 min were used for nitridation of four different samples. GaN was then overgrown at 1030 $^{\circ}\text{C}$ with constant TMGa and NH_3 flow rates of 156 $\mu\text{mol}/\text{min}$ and 7 l/min , respectively, maintaining a V/III ratio of 2000. The overall thickness was $\sim 7.5 \mu\text{m}$. For comparison, a control GaN layer was grown on the same GaN template using identical growth conditions but without the TiN network.

As suggested by the transmission electron microscope (TEM) analysis, thin and extended surface voids are formed above the discontinuous TiN layer, resulting in the lateral overgrowth of GaN.⁹ The TDs in the GaN template are blocked by the TiN layer, and many of the TDs penetrating through the TiN windows to the upper layer change their propagation direction and extend laterally. As a result density of threading dislocations significantly decreases at and above the TiN/GaN interface. From the X-Ray diffraction (XRD) results in Table 1 it is also seen that the full width at half maximum (FWHM) of the $(10\bar{1}2)$ peak decreases with increasing nitridation time. This generally suggests that the density of edge and mixed TDs is reduced with further nitridation. To ascertain whether the reduction of TDs actually reduces the nonradiative pathways, low temperature

photoluminescence (PL) and room temperature TRPL measurements were performed on all the samples.

Continuous-wave (cw) PL was measured at 10 K using a 25 mW HeCd laser operating at 325 nm (3.82 eV). Detection was performed by photon counting using a photomultiplier tube attached to a 1.25 m grating spectrometer. TRPL spectroscopy was employed at room temperature using a ~45 ps resolution Hamamatsu streak camera. Pulsed excitation was from a 1 kHz optical parametric amplifier with ~100 fs-wide pulses. The 3.82 eV excitation was incident 45° to the surface normal, and the TRPL was collected normal to the surface. The excitation density (~200 $\mu\text{J}/\text{cm}^2$) was kept well below the stimulated emission threshold to measure the decay times.

Figure 1 shows the 10 K PL spectra for the GaN epilayer samples with TiN subjected to 15 and 60 min nitridation and the control sample with no TiN. All of the samples (30 and 45 min nitridation samples not shown) exhibit strong excitonic features around the band edge. The blue and yellow luminescence bands are also visible but are as much as two orders of magnitude weaker than the bandedge emission in all the samples. An enlarged view of the band edge spectral region is shown in the inset of Figure 1, where the free exciton peaks at 3.491, 3.499, and 3.511 eV indicate the FX_A , the FX_B , and the FX_A excited state transitions, respectively. The main donor bound exciton (D^0X) emission is observed at 3.485 eV. The FWHM of the FX_A and the D^0X peaks obtained from Gaussian fits are given in Table 1. Another donor-bound exciton peak at 3.471 eV, which is not observed for the control sample, is visible for the samples with TiN network. The intensity of this peak is an order of magnitude larger for the 15 min nitridation sample than for other samples. We suspect that the number of Ti impurities in overgrown GaN is

reduced with increasing nitridation and that the 3.471 eV PL line may be related to these impurities.

To verify the excitonic peak assignments, temperature dependent PL measurements were performed on the 60 min nitridation sample. In the 300 K PL of Figure 2, the blue band disappears, the band edge emission redshifts to 3.422 eV, and the ratio of the band edge luminescence to the yellow luminescence decreases. The inset of Figure 2 shows the evolution of the FX_A peak with increasing temperature. Bound exciton peaks are visible up to 50 K, and only the FX_A and FX_B peaks remain above 100 K. The strong thermal quenching of the bound excitons comes from the increasing rate of excitation to the free exciton continuum.

The excitonic fine structure and the narrow linewidths at low temperatures are measures of the quality of samples; however, it is not possible to come to a conclusion about the radiative efficiency from cw-PL. TRPL is a nondestructive and powerful technique commonly used for characterization of excess carrier dynamics in semiconductors. Since most optical and electrical devices are operated at room temperature, understanding the fundamental excess carrier recombination dynamics at 300 K is required to evaluate the relevant radiative and nonradiative recombination mechanisms and thus to improve the performance of devices. The efficiency of the radiative recombination, and therefore the material quality, is strongly related to decay time of the particular transition. There is a limited number of reports related to the TRPL lifetimes of excess carriers in GaN at 300 K. Kwon *et al.*¹⁰ reported a biexponential decay with 150 and 740 ps time constants for high quality Si-doped MOCVD-grown GaN/sapphire. Decay times between 205-530 ps were measured for thick HVPE-grown templates,^{11,12,13} and

values ranging from 445¹⁴ to 506 ps¹³ were reported for homoepitaxially grown GaN layers. In addition, Chichibu *et al.*¹⁵ and Izumi *et al.*¹⁶ reported biexponential decays with lifetimes (t_1 , t_2) of (130, 400) ps and (80, 459) ps, respectively, for GaN/sapphire films grown using ELO. However, same groups obtained longer biexponential lifetimes of (130, 860) ps¹⁵ and (98, 722) ps¹⁶ for bulk GaN.

Figure 3 shows the TRPL data for the 15 min nitridation sample, the control sample, and a HVPE-grown 200 μm -thick freestanding GaN. The decays for all the samples were well characterized by a biexponential decay function: $A_1 \exp(-t/t_1) + A_2 \exp(-t/t_2)$. Table 1 summarizes the decay constants and the amplitude ratios (A_2/A_1) obtained from the fits using the Levenberg-Marquardt algorithm.¹⁷ The 15 min nitridation sample exhibits decay times that are the longest ever reported for GaN at room temperature.

Biexponential decays are characteristic of capture and recombination processes in a multilevel system. They may here be interpreted as related to the capture into deeper (nonradiative) centers, either in the bulk or at the surface/interface of the layer, followed by recombination. Although the biexponential decay times t_1 and t_2 most probably do not represent the pure nonradiative and radiative lifetimes, respectively, the ratio A_2/A_1 is suggestive of the relative importance of radiative decay. Thus, the particularly large ($A_2/A_1 > 0.5$) magnitude for the slow decaying components suggests increased radiative efficiency. Since the defect and the dislocation density may not be uniform, photoexcited area may contain two regions having different recombination times. Therefore, the measured lifetimes t_1 and t_2 are both limited by the nonradiative recombination.

With decreasing excitation energy density, the decay times slightly decreased [e.g. $(t_1, t_2) = (0.34 \text{ ns}, 1.60 \text{ ns})$ for $20 \mu\text{J}/\text{cm}^2$ excitation of the 15 min nitridation sample] for all the samples. The longer carrier lifetimes observed at higher photogenerated carrier densities may be attributed to the saturation of trap states.¹³ This will result in more carriers recombining through relatively slower band-to-band radiative recombination. Moreover, since both decay constants increase but A_2/A_1 remains constant [e.g. $A_2/A_1=0.55$ for $20 \mu\text{J}/\text{cm}^2$ excitation for the 15 min nitridation sample] with increasing excitation, we can also rule out the partial contribution from bimolecular recombination,¹⁶ which has an estimated characteristic decay time of around 1.6 ns for 10^{19} cm^{-3} carrier density.¹²

The improvement in decay times for the samples with TiN templates compared to the control GaN sample reflects the fact that TDs act as nonradiative recombination channels. However, no direct correlation is observed between the XRD linewidths and the decay times within the TiN network samples. For samples with a low density of TDs, it has been suggested that the very short diffusion length of carriers in GaN prevents most of the carriers from being trapped into TDs.¹⁵ Therefore, the observed sample-to-sample variation in the decay times may be ascribed to point defect-like nonradiative centers that cannot be detected by the TEM. Similar TRPL decay times measured from the wing and the window regions of ELO-GaN samples, which mainly have different TD densities, support this argument.^{15,16} These results indicate that threading dislocations do not limit the emission efficiency at room temperature as much as other types of nonradiative recombination centers like point defects and impurities.

In summary growth of GaN thin films on TiN micro-porous network templates significantly improves the structural quality and the radiative efficiency of the overgrown

layer. We believe that the time constants measured here for the GaN thin films with TiN templates are the longest ever reported for GaN at room temperature. The slow decaying component for the 15 min nitridation sample has a $t_2=1.86$ ns time constant that is comparable with the result of $t_2=1.73$ ns from a 200 μm -thick freestanding GaN, but has a relative magnitude (A_2/A_1) almost twice as large.

This work was supported by a DURINT program administered by ONR (Dr. C. E. C. Wood). The research also benefited from grants from AFOSR (Dr. T. Steiner and Dr. G. L. Witt). The Duke portion of this work was funded in part by U.S. Army Research Office Grant DAAG55-98-D-0002. The authors would like to thank Profs. R. M. Feenstra of Carnegie Mellon, T. S. Kuan of SUNY Albany, and D. J. Smith of Arizona State University for their critical contributions to the development of TiN nanonetwork based GaN by MOCVD.

TABLES:

Table 1: XRD and 10 K PL linewidths, and TRPL decay constants and amplitude ratios (at 200 $\mu\text{J}/\text{cm}^2$ excitation density) for GaN thin layer samples grown on TiN templates. Data for the control sample with no TiN layer and a freestanding GaN sample are also included.

Sample	FWHM $\text{FX}_A, \text{D}_0\text{X}$ (meV)	XRD (0002), (10 $\bar{1}$ 2)		t_1, t_2 (ns)	A_2/A_1
		(arcmin)			
15 min	3.22, 3.90	6.43, 6.11		0.47, 1.86	0.59
30 min	3.88, 4.52	5.83, 4.86		0.39, 1.32	0.58
45 min	4.00, 5.27	5.09, 4.61		0.45, 1.68	0.54
60 min	3.40, 3.24	4.97, 4.57		0.41, 1.54	0.52
Control	3.09, 3.15	5.60, 7.11		0.13, 0.30	0.36
Freestanding GaN				0.34, 1.73	0.33

FIGURES:

Figure 1: 10 K PL spectra for the 15 min and 60 min nitridation samples and the control sample. The inset shows the free exciton region of the spectra.

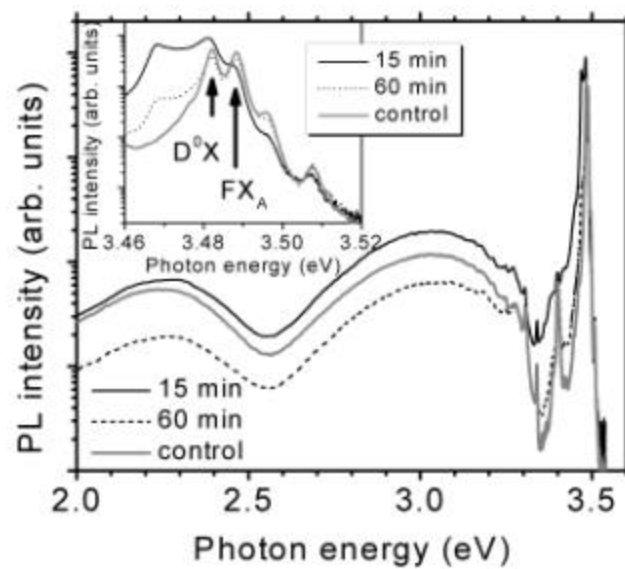
Figure 2: Room temperature PL spectrum for the 60 min nitridation sample. The inset shows the temperature dependence of the free exciton region. The peaks marked with filled circles show the evolution of the A-free exciton (FX_A) peak.

Figure 3: Normalized time-resolved PL spectra for the 15 min nitridation sample, control sample, and freestanding GaN. The solid lines are biexponential fits to the data.

Ü. Özgür *et al.*

Appl. Phys. Lett.

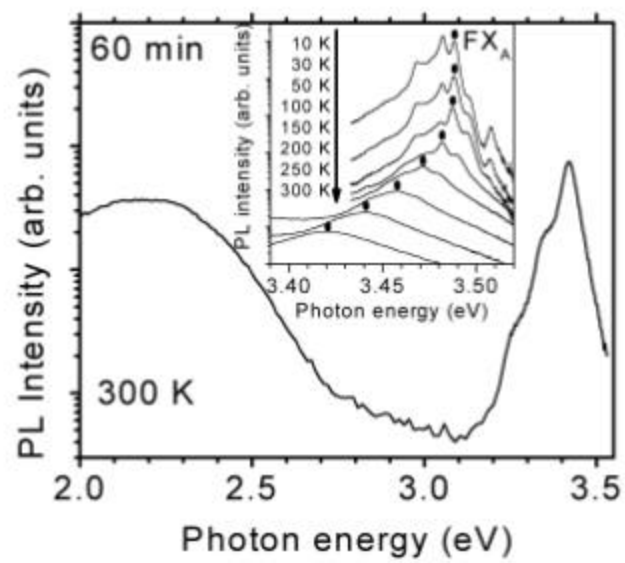
Figure 1



Ü. Özgür *et al.*

Appl. Phys. Lett.

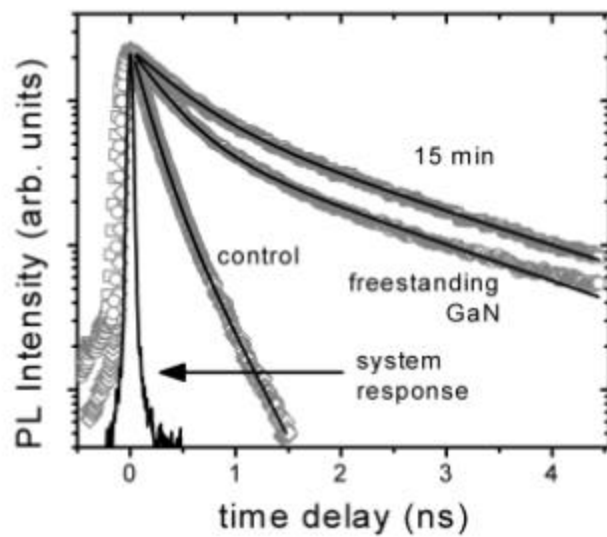
Figure 2



Ü. Özgür *et al.*

Appl. Phys. Lett.

Figure 3



References:

-
- ¹ H. Morkoç, “*Nitride Semiconductors and Devices*”, Springer-Verlag (1999).
 - ² M. A. Reshchikov and H. Morkoç, “Defects in GaN: Optical Signature”, *J. Appl. Phys. Reviews*, submitted.
 - ³ P. Visconti, K. M. Jones, M. A. Reshchikov, F. Yun, R. Cingolani, H. Morkoç, S. S. Park, and K. Y. Lee, *Appl. Phys. Lett.*, **77**, 3743, (2000).
 - ⁴ Y. Oshima, T. Eri, M. Shibata, H. Sunakawa, and A. Usui, *Phys. Stat. Sol. (a)* **194**, No. 2, 554 (2002).
 - ⁵ See for example, P. Gibart, B. Beaumont, P. Vennéguès, “Epitaxial Lateral Overgrowth of GaN” in “*Nitride Semiconductors, Chapter 2 in Handbook on Materials and Devices*” Eds. P. Ruterana, M. Albrecht and J. Neugebauer, Wiley-VCH GmbH & Co.KgaA, Weinheim, ISBN: 3-527-40387-6 (2003).
 - ⁶ S. Haffouz, B. Beaumont, P. Vennegues, and P. Gibart, *Phys. Status Solidi (a)* **176**, 677 (1999).
 - ⁷ S. Sakai, T. Wang, Y. Morishima, and Y. Naoi, *J. Cryst. Growth* **221**, 334 (2000).
 - ⁸ A. Sagar, R. M. Feenstra, C. K. Inoki, T. S. Kuan, Yi Fu, Y. T. Moon, H. Morkoç, International Workshop on Nitride Semiconductors, Pittsburgh USA 2004, and *Phys. Stat. Sol.* in press.
 - ⁹ Y. Fu, Y. T. Moon, F. Yun, Ü. Özgür, J. Q. Xie, S. Dogan, H. Morkoç, C. K. Inoki, T. S. Kuan, L. Zhou and D. J. Smith, accepted to *Appl. Phys. Lett.* (2004).
 - ¹⁰ Ho Ki Kwon, C. J. Eiting, D. J. H. Lambert, M. M. Wong, R. D. Dupuis, Z. Liliental-Weber, and M. Benamara, *Appl. Phys. Lett.* **77**, 2503 (2000).

-
- ¹¹ G. E. Bunea, W. D. Herzog, M. S. Ünlü , B. B. Goldberg, and R. J. Molnar, Appl. Phys. Lett. **75**, 838 (1999).
- ¹² S. Juršenas, I. S. Miasojedovas, G. Kurilcik, A. Žukauskas, and P. R. Hageman, Phys. Stat. Sol. (a) **201**, 199 (2004).
- ¹³ A. V. Sampath, G. A. Garrett, C. J. Collins, P. Boyd, J. Choe, P. G. Newman, H. Shen, M. Wraback, R. J. Molnar, and J. Caissie, J. Vac. Sci. Technol. B **22**, 1487 (2004).
- ¹⁴ S. Juršenas, N. Kurilcik, G. Kurilcik, A. Žukauskas, P. Prystawko, M. Leszcynski, T. Suski, P. Perlin, I. Grzegory, and S. Porowski, Appl. Phys. Lett. **78**, 3776 (2001).
- ¹⁵ S. F. Chichibu, H. Marchand, M. S. Minsky, S. Keller, P. T. Fini, J. P. Ibbetson, S. B. Fleischer, J. S. Speck, J. E. Bowers, E. Hu, U. K. Mishra, S. P. DenBaars, T. Deguchi, T. Sota, S. Nakamura, Appl. Phys. Lett. **74**, 1460 (1999).
- ¹⁶ T. Izumi, Y. Narukawa, K. Okamoto, Y. Kawakami, Sg. Fujita, S. Nakamura, J. Lumin. **87-89**, 1196 (2000).
- ¹⁷ W. H. Press, B. P. Flannery, S. A. Teukolsky, and W. T. Vetterling, *Numerical Recipes in C: The Art of Scientific Computing*, Cambridge University Press, Cambridge (1988).